

European Geosciences Union
General Assembly 2012

Vienna, Austria,
22 - 27 April 2012

Session HS7.4/AS4.17/CL2.10:
Climate, Hydrology and
Water Infrastructure

Long term properties of monthly atmospheric pressure fields

Savvas Giannoulis, Christos Ioannou, Emmanouil Karantinos,
Lamprini Malatesta, Georgios Theodoropoulos, Georgios Tsekouras,
Anna Venediki, Panayiotis Dimitriadis, Simon Michael Papalexiou
and Demetris Koutsoyiannis

Department of Water Resources and Environmental Engineering,
National Technical University of Athens, Greece

1. Abstract

We assess the statistical properties of atmospheric pressure time series retrieved from a large database of monthly records. We analyze the short and long term properties of the time series including possible trends, persistence and anti-persistence. We also analyze time series of climatic indices which are based on the atmospheric pressure fields, such as the North Atlantic oscillation index and the El Niño-Southern Oscillation index.

Acknowledgment: This research is conducted within the frame of the undergraduate course “Stochastic Methods in Water Resources” of the National Technical University of Athens (NTUA). The School of Civil Engineering of NTUA provided support for the participation of the students in the Assembly.

2. Data set

We retrieve monthly time series of sea-level atmospheric pressure fields from “KNMI Climate Explorer”. To explore long-term climatic variability, we only analyse stations with a record length of at least eighty years, a total of 103 stations.

Moreover, we collect pressure-related time series concerning climate indices of the North Atlantic oscillation and the El-Niño Southern oscillation. The North Atlantic oscillation index is based on the difference of normalized sea level pressures between Lisbon(Portugal), Ponta Delgada (Azores) and Stykkisholmur/Reykjavik(Iceland). The El-Niño Southern oscillation index is defined as the normalized pressure difference between Tahiti, French Polynesia and Darwin, Australia.

The table below shows the characteristics of the time series used.

	North Atlantic oscillation		El-Niño Southern oscillation			
	station based	reconstructed	station based	station based	reconstructed	reconstructed
Time series period	1864-2011	1659-2001	1866-2010	1882-2008	900-2002	1706-1977
Time step	annual	annual	monthly	monthly	annual	annual
Source	KNMI Climate Explorer	NASA	KNMI Climate Explorer		NASA	

3. Summary of statistical characteristics

Number of stations per class of sample size and per continent

Continent	70-80	81-90	91-100	101-110	111-120	121-130	131-140	141-150	151-160	161-170	171-240	TOTAL
EUROPE	1	4	3	0	1	2	3	2	2	0	4	22
AFRICA	2	1	0	0	0	0	0	0	0	1	0	4
ASIA	0	4	6	10	0	0	0	1	0	0	1	22
OCEANIA	0	3	3	2	3	2	2	1	0	0	0	16
AMERICA	3	12	9	7	3	3	0	0	0	0	0	37
ANTARCTICA	0	0	1	0	0	0	0	0	0	0	0	1
TOTAL	6	24	22	19	7	7	5	4	2	1	5	102

Range of statistical characteristics per continent

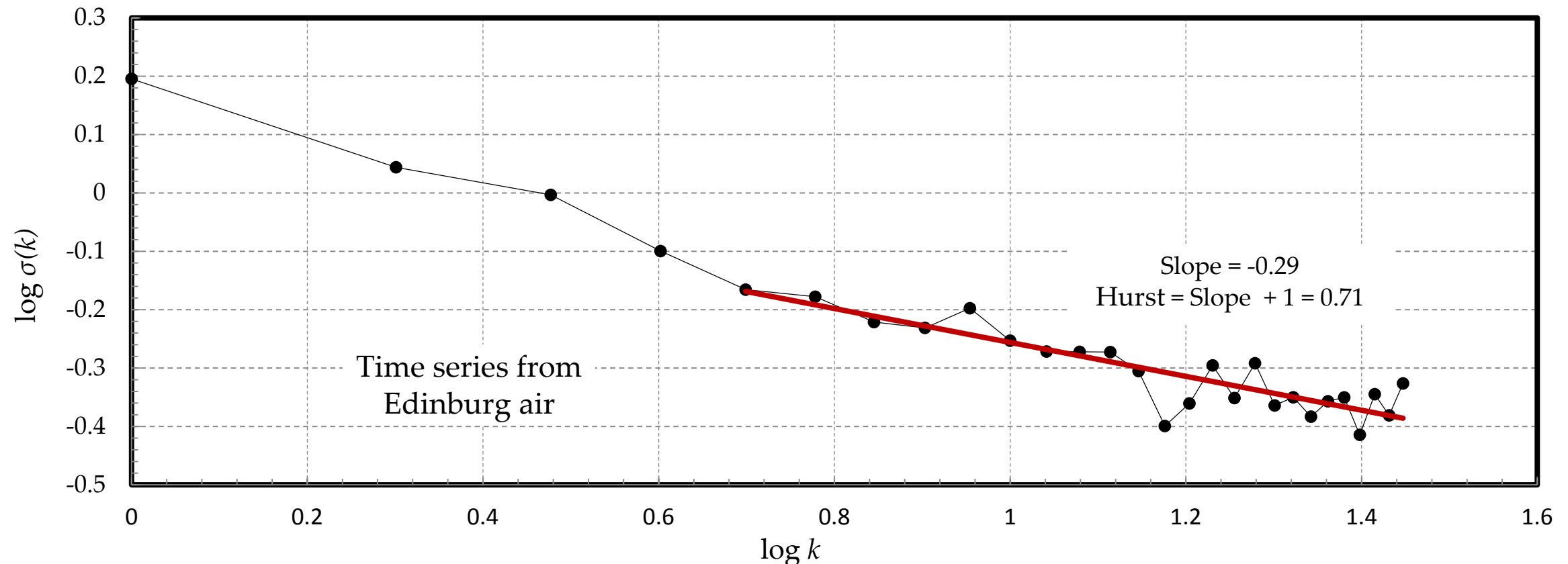
		EUROPE	AFRICA	ASIA	OCEANIA	AMERICA	ANTARCTICA
MEAN	min	1005,4	1013,9	1007,02	1009,1	1005,78	992,1
	max	1021,43	1017,34	1010,86	1017,16	1019,25	992,1
STANDARD DEVIATION	min	0,72	0,47	0,4	0,63	0,51	1,51
	max	2,22	1,19	1,17	2,71	2,43	1,51
SKEWNESS COEFFICIENT	min	-0,5	-0,22	-1,83	-0,39	-1,28	0,73
	max	0,46	0,74	0,53	0,99	1,07	0,73
AUTOCORRELATION FOR UNIT LAG	min	-0,07	0,08	0,27	-0,03	0,05	-0,09
	max	0,66	0,87	0,89	0,75	0,89	-0,09
HURST COEFFICIENT	min	0,36	0,48	0,1	0,43	0,51	0,51
	max	0,91	0,98	0,98	0,95	0,98	0,51
MINIMUM VALUE	min	999,99	1013	1004	1005,2	1000,9	989,25
	max	1018,34	1016,22	1009,15	1014,59	1016,59	989,25
MAXIMUM VALUE	min	1009,56	1015,19	1008,55	1011,38	1010,21	997,44
	max	1024,42	1019,44	1013,13	1020,78	1022,06	997,44

4. Methodology 1

The monthly time series are converted into annual time series. In cases where more than 4 monthly values were missing, the annual average for that year was omitted.

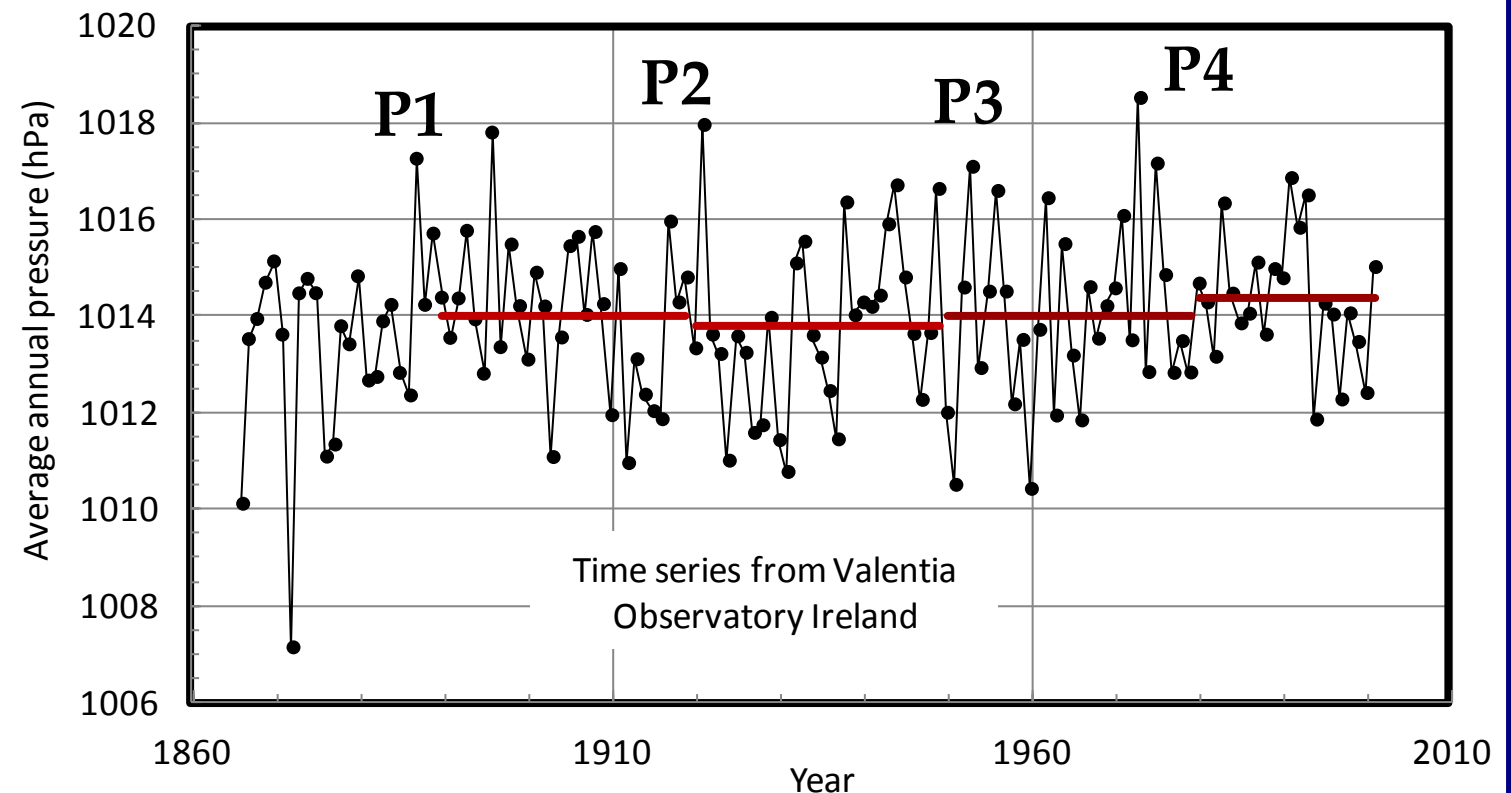
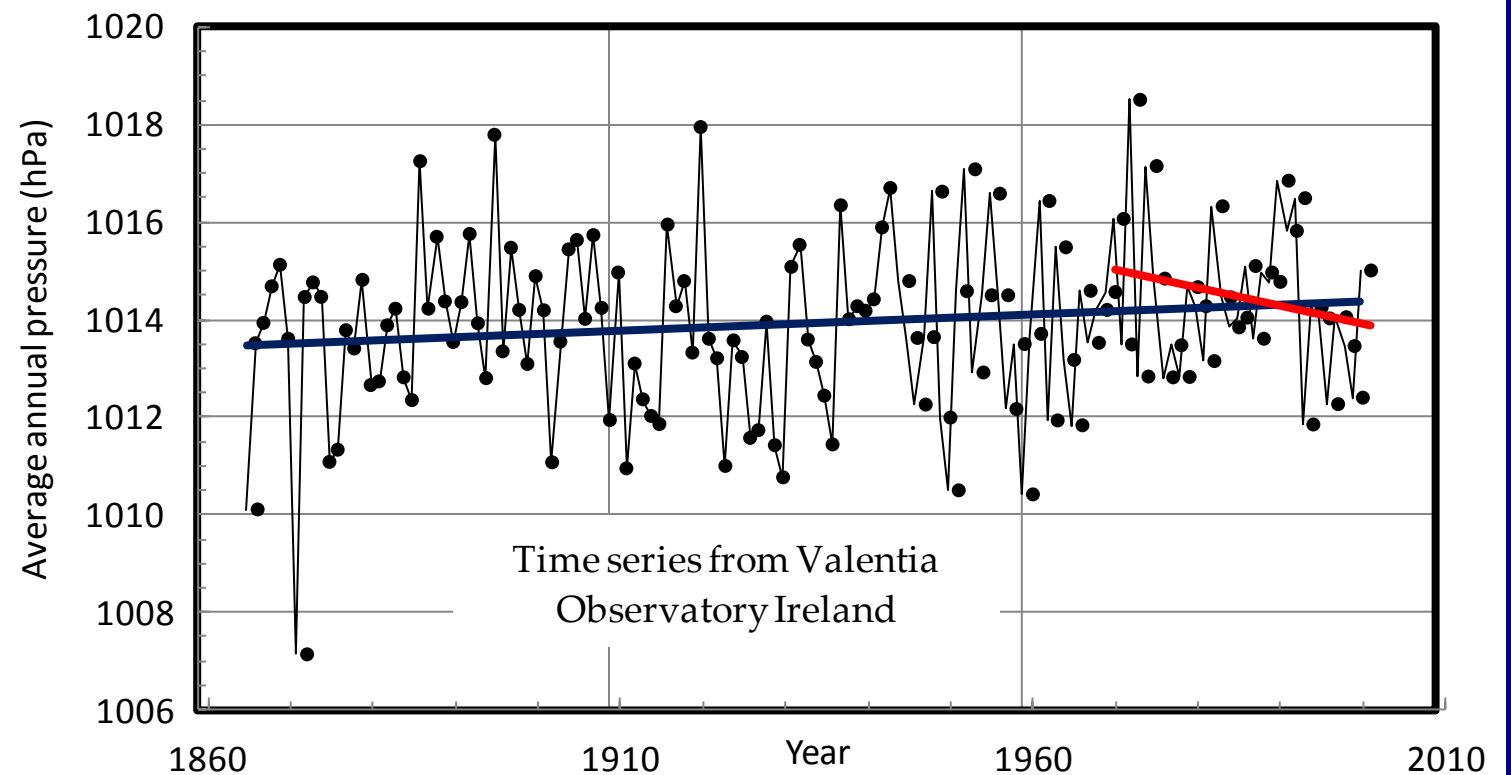
The persistence is examined by estimating the Hurst coefficient. Based on the simple scaling stochastic process (SSS process), we create a double logarithmic plot of standard deviation $\sigma(k)$ versus time scale k for each time series. The Hurst coefficient derives from the slope of the diagram (Koutsoyiannis 2005).

To convert the annual time series into time series of averages at scale k and then estimate $\sigma(k)$, a value at scale k is estimated if less than one third of the annual values are missing.



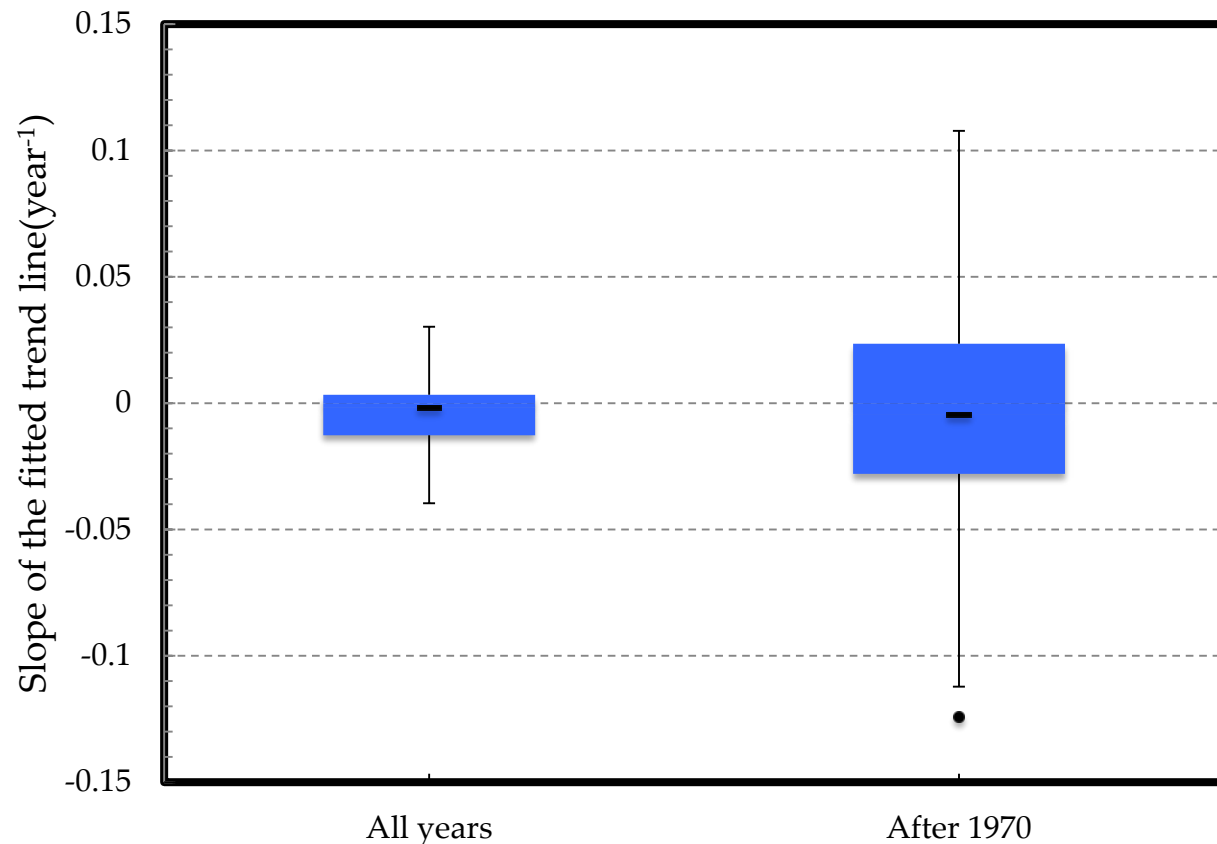
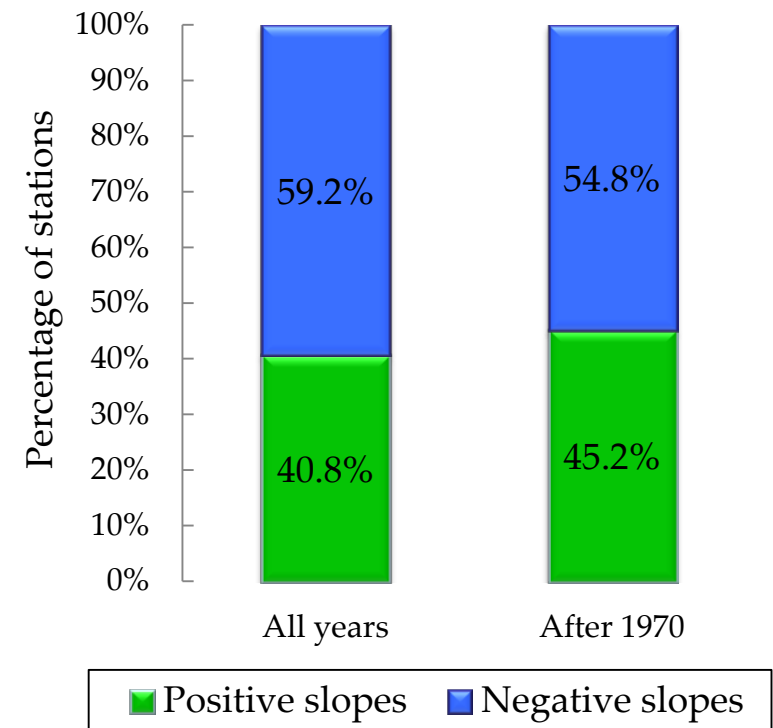
5. Methodology 2

- In addition, trends are examined:
 - For the whole time series (blue line on figure on the right)
 - For the part of the time series from 1970 up to the latest record (red line on figure on the right)
- The time series of the sea-level atmospheric pressures are split in thirty-year periods (P1: 1890-1920; P2: 1920-1950, P3:1950-1980, P4:1980-2010).
- Climatic (30-year) means and standard deviations are calculated for each of the four periods.
- In order to make comparable the trends and the differences between standard deviations, the times series are standardized by the standard deviation of the entire series, which varies from 0.4 to 8.2 hPa



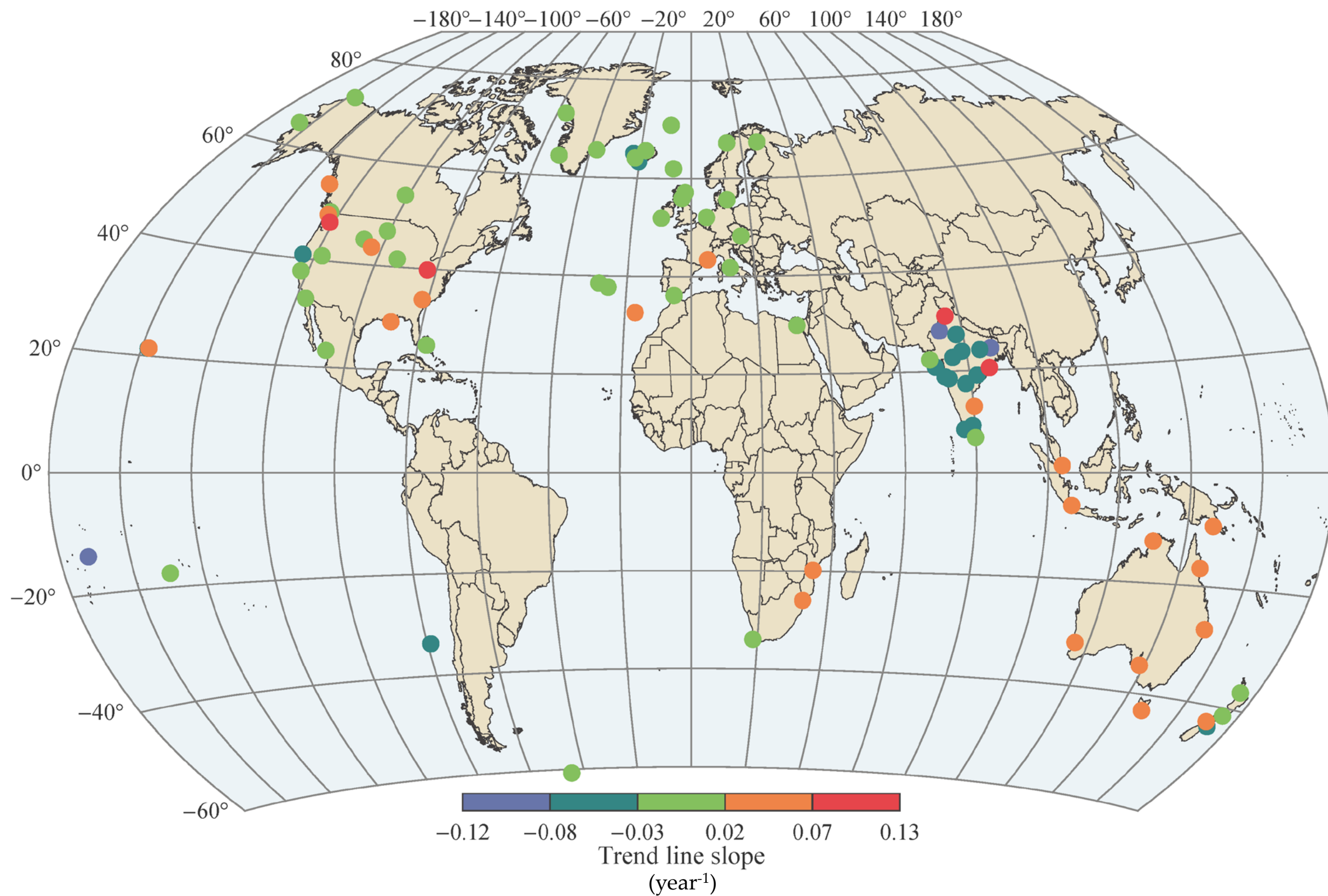
6. Results of trend analysis

The chart on the right depicts the proportion of upward and downward trends, for both the entire period and the period from 1970 and thereafter. We notice that the percentage of increasing trends is lower than that of the decreasing trends.



The chart on the left depicts the box plots of slopes for both the entire period and the period from 1970 and thereafter. The length of each whisker equals one and a half of the interquartile range

7. Geographical variation of the trends after 1970

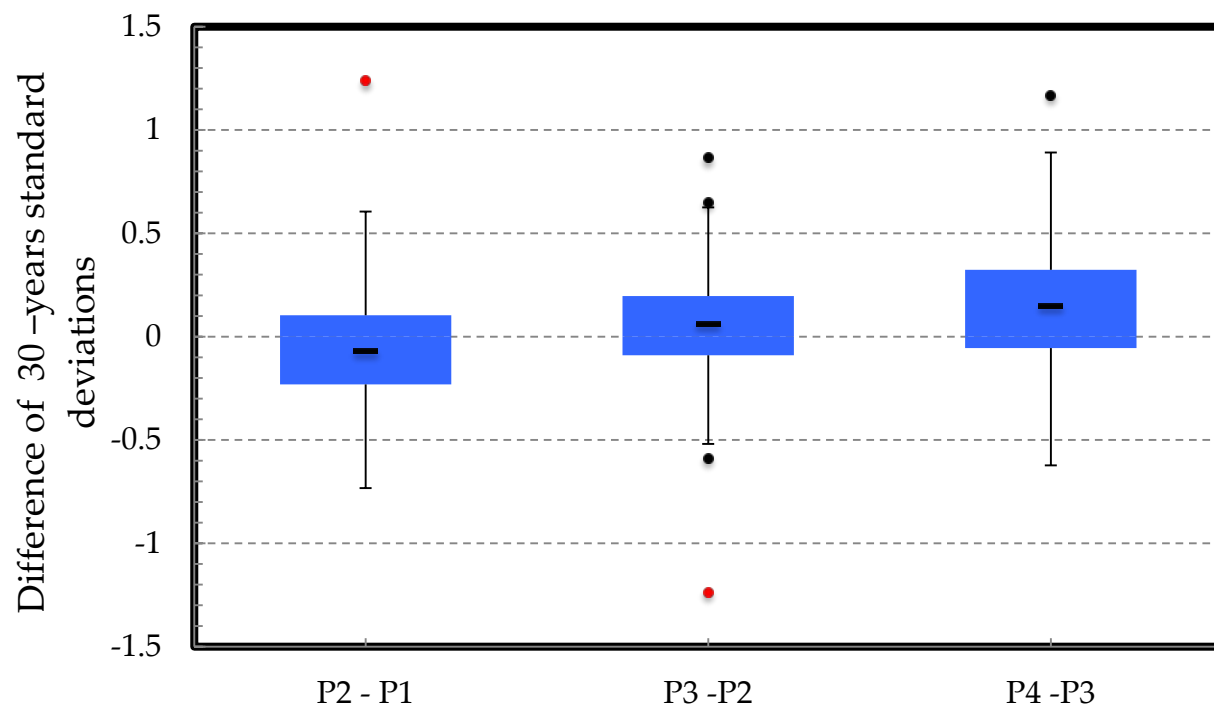
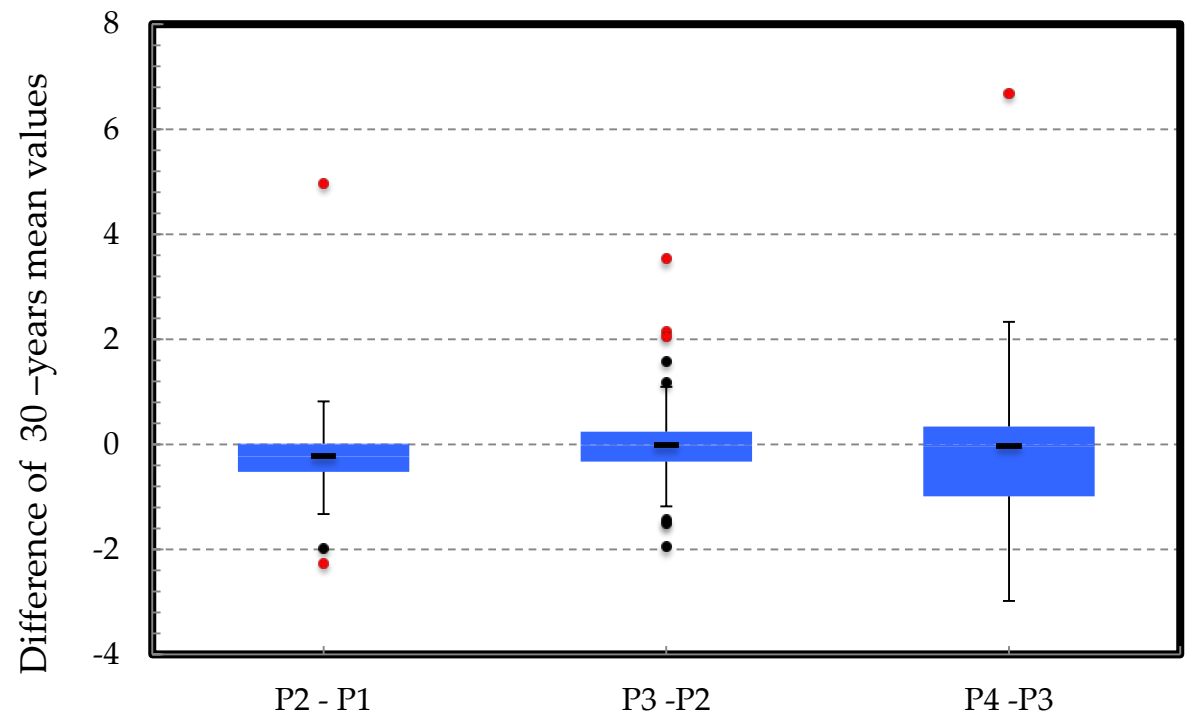


8. Differences of climatic means and standard deviations in consecutive 30-year periods

P2-P1/P3-P2: In both cases, we notice that there is an insignificant difference between the means of the two consecutive periods.

P4-P3: There is a substantially wider range of the differences between the means of the two consecutive periods. Moreover, a negative skewness is observed.

In all cases, the median is close to zero.



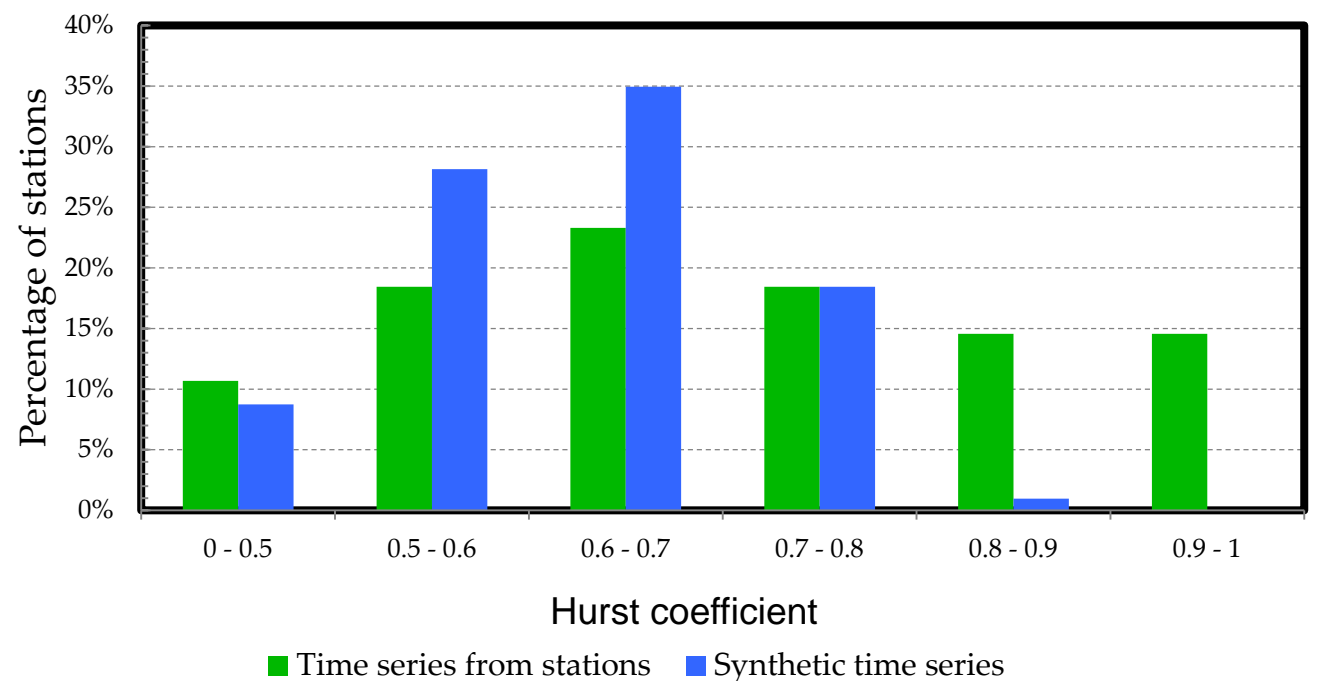
The standard deviation is characterized by a gradual increase throughout the latest three 30-year periods.

Moreover, the range of standard deviation differences is noticeably wider in the latest period.

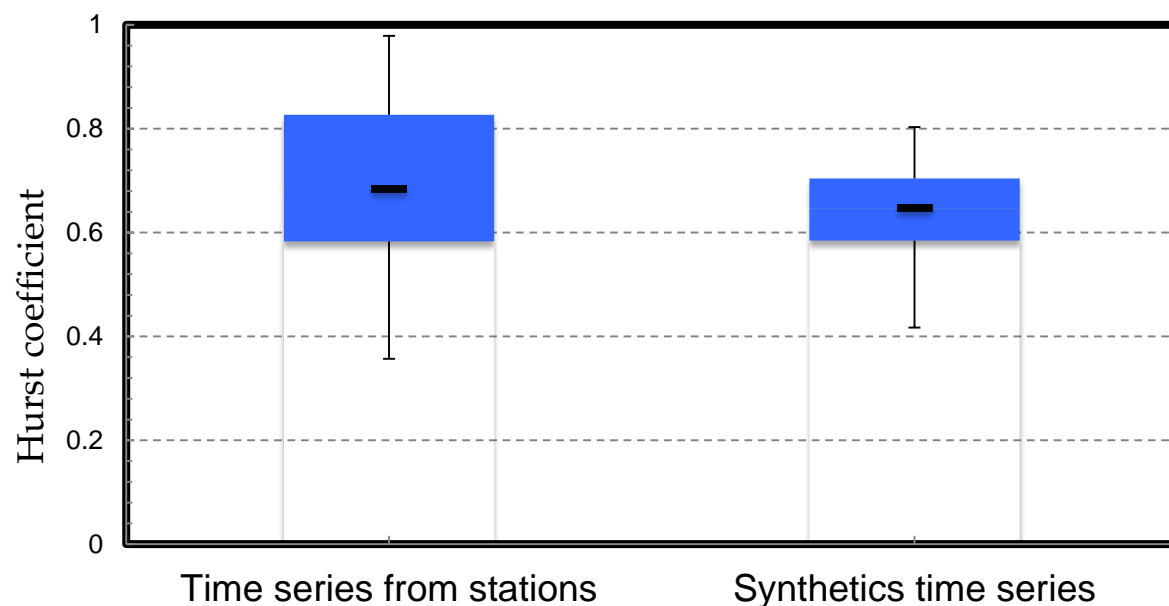
*the length of each whisker equals one and a half of the interquartile range

9. Analysis of the Hurst coefficient

The chart on the right depicts the histogram of the Hurst coefficient, estimated from station time series. We observe that the Hurst coefficient for the vast majority of the time series exceeds 0.5. A small percentage of Hurst coefficients below 0.5 can be attributed to statistical sampling; to show this we compare with a histogram of synthetic time series generated by the multiple timescale fluctuation approach (Koutsoyiannis 2002) using the average Hurst coefficient. The Hurst coefficients ranging from 0 to 0.5 in both types of time series have a similar percentage. The probability density functions diverge significantly for values ranging from 0.8 to 1.



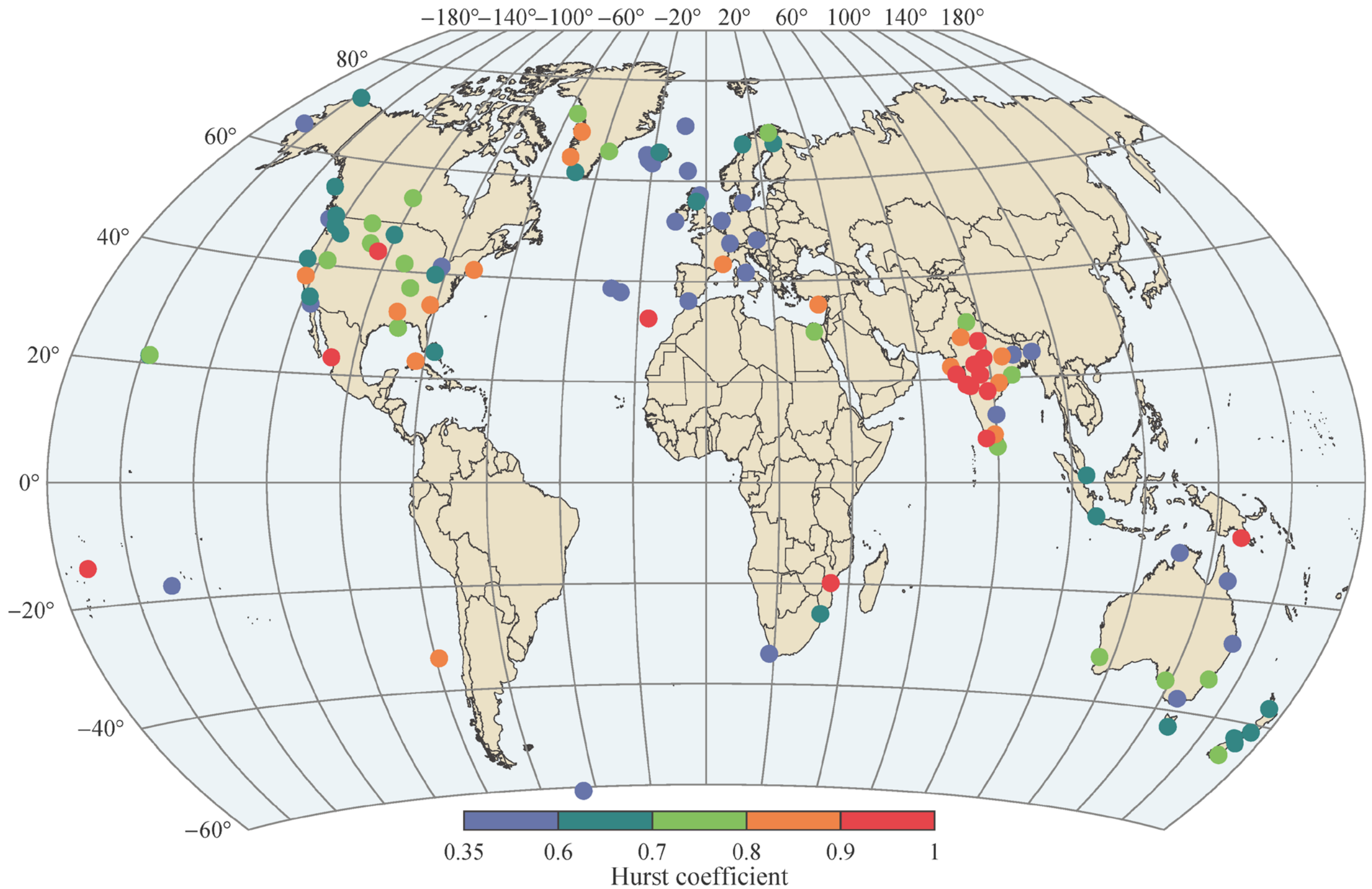
From the box plot of Hurst coefficients, we observe the following:



- The values of the Hurst coefficient from the observations are clustered between 0.58 and 0.83 while the values deriving from the synthetic time series accumulate between 0,42 and 0,80.
- The range of the Hurst coefficient from the observations is wider than the range from the synthetic time series.

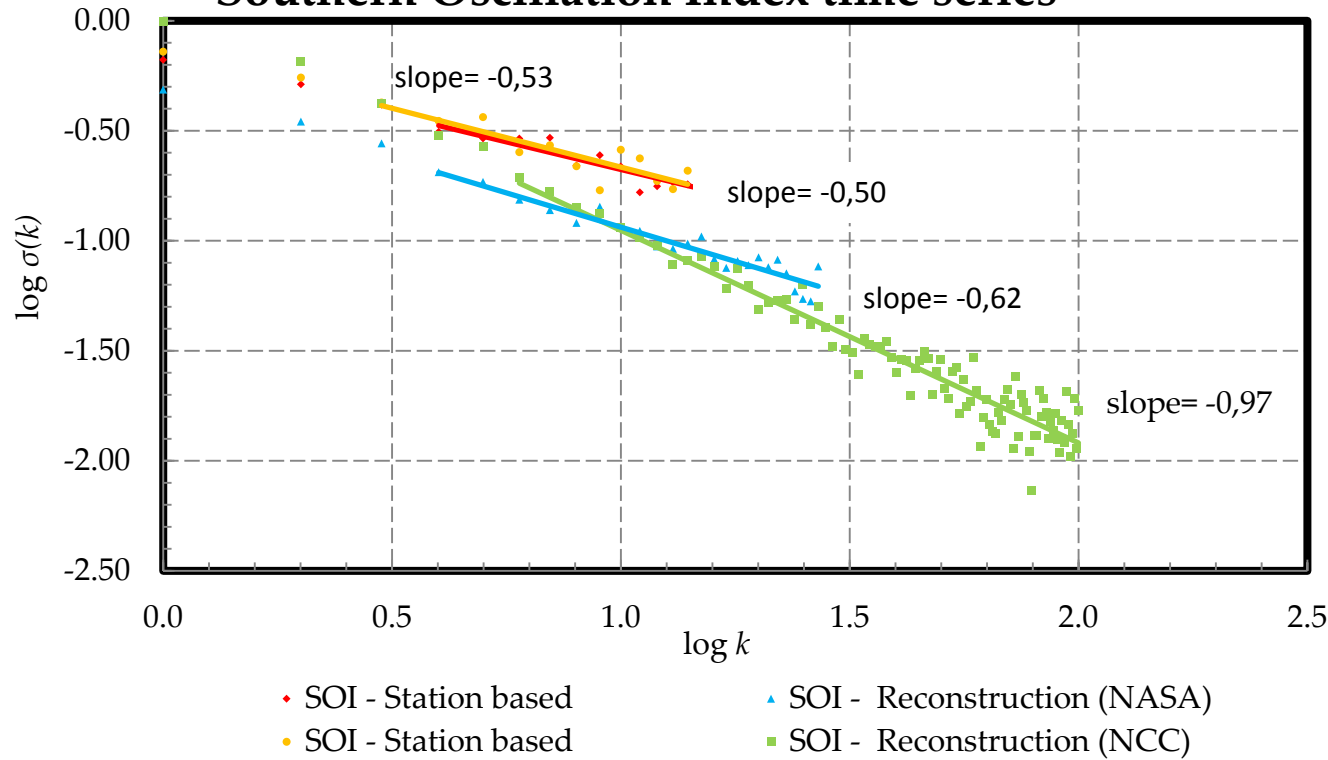
* the end of each whisker represents the maximum and minimum value

10. Geographical variation of Hurst coefficient



11. North Atlantic and El Niño-Southern Oscillation indices analysis

Southern Oscillation Index time series



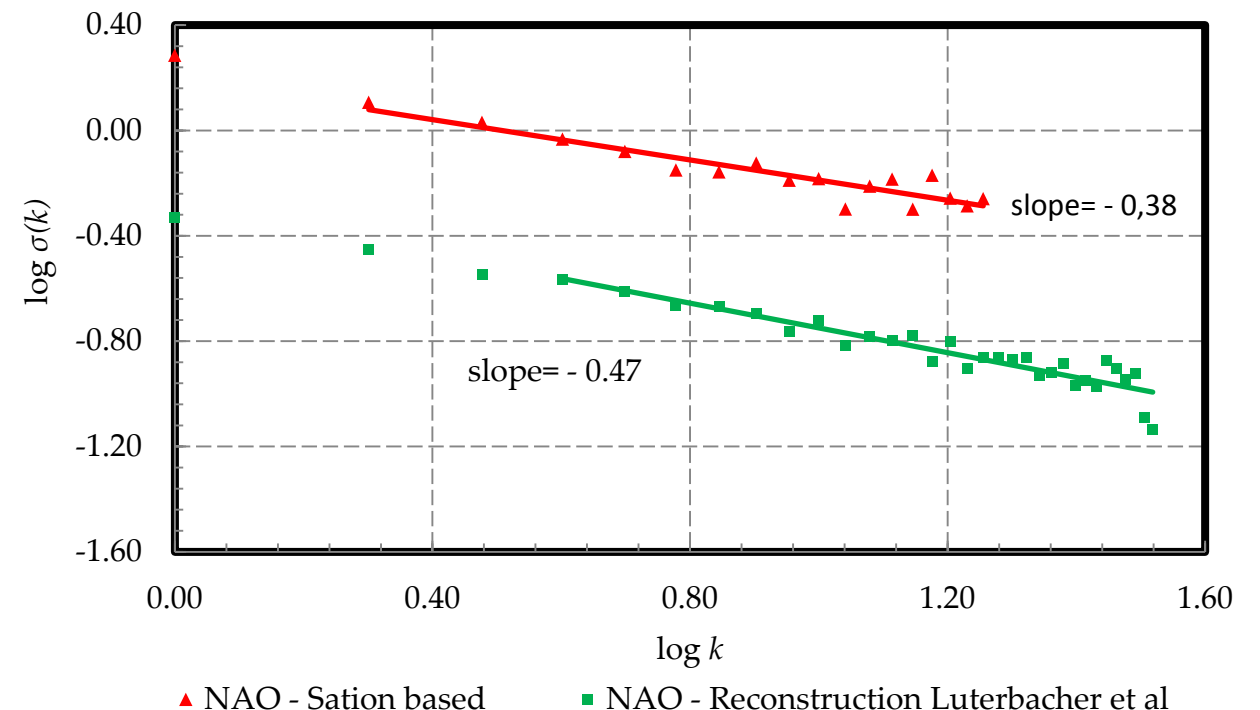
The graph on the left illustrates the climacogram ($\log(\sigma(k))$ versus $\log(k)$) for each of the SOI time series examined. The stations related to the SOI are presented in the table below.

Station	Hurst
Darwin	0,58
Tahiti	0,37

The graph on the right illustrates the climacogram for each of the examined NAO indices. The slope value of the station based time series indicate a slightly persistent behaviour. The stations related to the North Atlantic Oscillation Index are presented below:

Station	Hurst
Ponta Nelgada	0,60
Reykjavic	0,47
Stykkisholmur	0,53

North Atlantic Oscillation Index time series



* Lisbon's Hurst was not assessed due to insufficient data (30-year records)

12. Conclusions

- From the analysis of both trends and aggregated time series of sea-level atmospheric pressure on climatic (30-year) scale, the percentage of downward trends is slightly higher than of upward trends. A worldwide consistent trend cannot be asserted.
- Sea level atmospheric pressures indicate the existence of Hurst-Kolmogorov behaviour with a mean value of ~ 0.7 . A small percentage of Hurst coefficients below 0.5 can be attributed to sampling errors. It is quite interesting that some of the time series are characterized by very high values of Hurst coefficient (> 0.9) that depart significantly from the mean value.
- The analyses for the El Niño-Southern oscillation and the North Atlantic oscillation indices do not confirm a persistent behaviour and the results are not conclusive. The NCC reconstruction of El Niño-Southern oscillation index suggests strong antipersistence ($H = 0.03$) but this does not agree with the station based time series.

References

- KNMI Climate Explorer monthly sealevel_pressure stations between -90N to 90N and -180E to 180E, <http://climexp.knmi.nl/getstations.cgi>
- KNMI Climate Explorer SOI (Southern Oscillation Index) from Climatic Research Unit, <http://climexp.knmi.nl/getindices.cgi?WMO=CRUDData/soi&STATION=SOI&TYPE=i&id=someone@somewhere>
- KNMI Climate Explorer 1,100 Year El Niño/Southern Oscillation (ENSO) Index Reconstruction, Li et al 2011.
- http://climexp.knmi.nl/getindices.cgi?WMO=RapidData/enso_li&STATION=Li_ENSO&TYPE=i&id=someone@somewhere&NPERYEAR=1
- Koutsoyiannis, D., The Hurst phenomenon and fractional Gaussian noise made easy, *Hydrological Sciences Journal*, 47 (4), 573–595, 2002.
- Koutsoyiannis, D., Uncertainty, entropy, scaling and hydrological stochastics, 2, Time dependence of hydrological processes and time scaling, *Hydrological Sciences Journal*, 50 (3), 405–426, 2005.
- Luterbacher et al NAO Reconstructions
- <http://www.cru.uea.ac.uk/cru/data/paleo/naojurg/>
- NAO Index Data provided by the Climate Analysis Section, NCAR, Boulder, USA, Hurrell (1995). Updated regularly. Accessed 01 January 2012, <http://climatedataguide.ucar.edu/guidance/hurrell-north-atlantic-oscillation-nao-index-station-based>
- NASA Goddard Space Flight Center Southern Oscillation Index (SOI) Reconstruction
- http://gcmd.nasa.gov/KeywordSearch/Metadata.do?Portal=GCMD&KeywordPath=Parameters%7CPALEOCLIMATE%7CLAND+RECORDS%7CTREE+RING&OrigMetadataNode=GCMD&EntryId=NOAA_NCDC_PALEO_1998-038&MetadataView=Full&MetadataType=0&lbnode=mdlb3
- University Corporation for Atmospheric Research, Climate analysis section <http://www.cgd.ucar.edu/cas/catalog/climind/soi.html>